Parametric Stability and Failure Mechanisms of Silicon Carbide Pressure Sensors

R.S. Okojie[1], P. Nguyen[2], V. Nguyen[2], E. Savrun[2], D. Lukco[3], J. Buehler[3], and T. McCue[3], S. Knudsen[4]
[1]NASA Glenn Research Center, Cleveland, OH, USA
[2]Sienna Technologies, Inc. Woodinville, WA, USA
[3]QSS Group, Inc. Cleveland, OH, USA
[4]Sandia National Labs, Albuquerque, NM, USA
Email: robert.s.okojie@nasa.gov

Abstract

We have performed in-depth failure analysis (FA) on SiC pressure transducers and identified the mechanisms responsible for their failures. The pressure sensors were packaged using the MEMS Direct Chip Attach (MEMS-DCA) technique in which the wire bond process is eliminated. Accelerated Stress Test (AST) that was developed specifically for high temperature operating devices was initially performed to extract the stable operating characteristics of the transducers, which allowed for extracting the operating parameters and rating of their highest operating pressure and temperature. After the AST that included several hours of cyclic pressure and temperature excursions, the recorded maximum drift of the zero pressure offset voltage at room temperature, V_{oz}(25 ^{o}C), was 1.9 mV, while the maximum drift at 500 ^{o}C was 2.0 mV. The maximum recorded drift of the full-scale pressure sensitivity after ten hours of thermal cycling at 500 ^{o}C was ± 1 μV/V/psi. In almost all cases, the observed failures during field validation were associated with the detachment of the die-attach material from the sensor bondpads.

Key words: Silicon carbide, High Temperature, Pressure Sensor, Failure Analysis, and Reliability.

1.0 Introduction

Pressure monitoring during deep well drilling, in automobiles and jet engines requires pressure sensors that can operate for a long time (>10,000 hrs) and reliably at temperatures between 200 ^{o}C and 600 ºC [1, 2]. Conventional silicon semiconductor pressure transducers increasingly suffer from instability and failure as the operation is extended toward the higher temperature range. The reasons include the degradation of metal/semiconductor electrical contacts and weakening of wire bond interface with the bondpad due to temperature-driven intermetallic diffusion [3]. Therefore, in order to extend the silicon pressure sensor operating temperature, complex and costly packaging schemes that include plumbing with water or nitrogen are implemented to maintain reliable and accurate operation. The complexity and high cost that are associated with such schemes are further compounded by increase in weight, volume, additional connections, and the increasing difficulty to access the environment.

Silicon Carbide (SiC) semiconductor pressure sensors have been previously demonstrated to operate at temperatures up to 600 ^{o}C [4]. Recently, the demonstration of leadless (no wire bond) SiC-based pressure transducers operating at 500 ^{o}C were reported by two groups [5, 6]. The flip-chip inspired approach and elimination of the wire bonds has greatly helped to protect the metallization from the harsh environment, thereby offering the potential for long-term survival of SiC pressure transducers at high temperature. These developments have increased the possibility of direct insertion of un-cooled SiC pressure sensors into high temperature environments. However, for SiC pressure sensor technology to transition from the laboratory to commercial production, several reliability challenges, including package-induced stress and metal contact degradation, must be resolved. To be commercially viable, these sensors must undergo appropriate Failure Analysis (FA). There also is the need to develop reliability testing standards that are specific to harsh environment microsystems. The existing Joint Electron Device Engineering Council reliability testing standards are only applicable to conventional-environment semiconductor microsystems [7]. Due to the absence of a testing standard for high

temperature MEMS, we had previously developed and adopted an Accelerated Stress Testing (AST) protocol to evaluate the reliability performance of packaged SiC pressure transducers under cyclic pressure and temperature [8]. The AST protocol used in [8] is reproduced in Figure 1 and its complete description can be found in that publication.

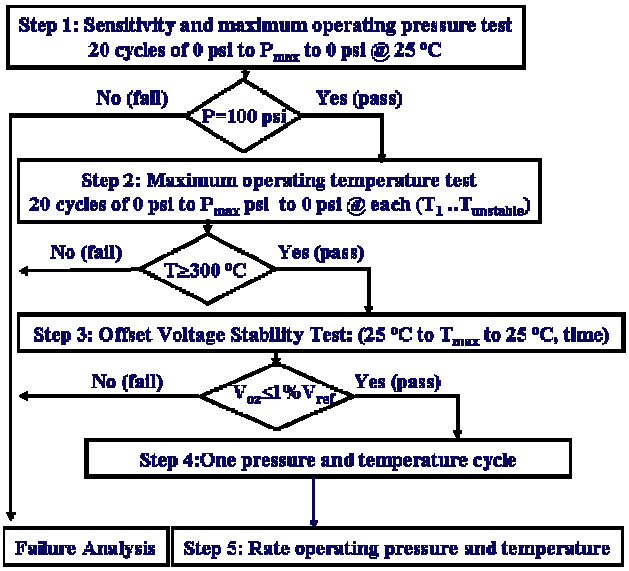

Figure 1: The AST protocol for evaluating the long term reliability of SiC pressure sensors at high temperature [8].

2.0 Stability of transducer parameters

In this work, only four of the six SiC transducers evaluated survived through Step 4 of the AST shown in Figure 1. The passing transducers were then rated in terms of their maximum operating pressure and temperature and then sent to Sandia National Laboratory for field validation. For the AST qualified transducers, two were rated at T_{max} of 400 °C while the other two were rated at 500 °C. The rated maximum operating pressure in all cases was 500 psi. The full-scale output voltage, V_{fso}, of the two transducers rated at 400 °C (#s 63 and 64) is shown in Figure 2a, as recorded during the last testing sequence at the end of Step 4 of the AST protocol. In terms of the trend in performance characteristics, the similarity in the V_{fso} between the two transducers is quite evident. It can also be observed that the output of the transducers decreases with temperature. This is an indication of the loss of strain sensitivity with increasing temperature, as is further evidenced in Figured 2b. This behavior is characteristic of piezoresistive sensors. The strain sensitivity at 400 °C as plotted in Figure 2b shows that the transducers still retained about 60% of their room temperature values.

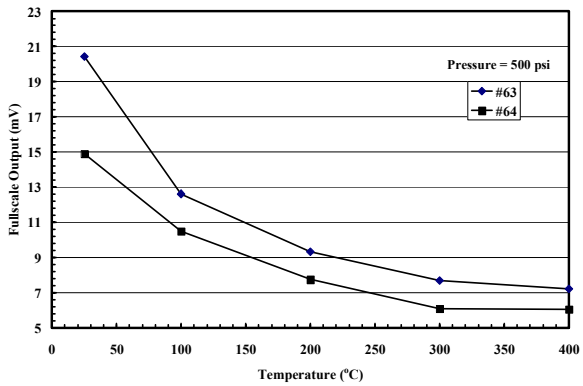

Figure 2a: Full-scale output at 500 psi as function of temperature of two transducers during final step 4 sequence of the AST protocol.

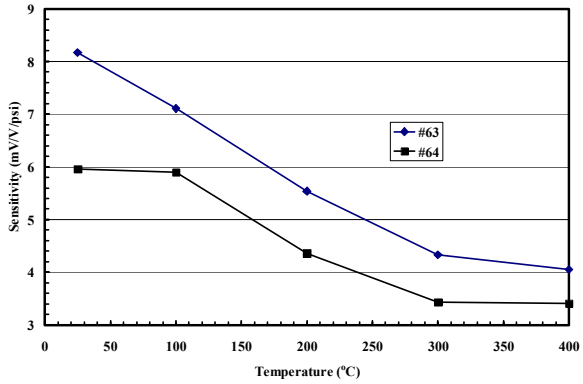

Figure 2b: Effect of temperature on the strain sensitivity after step 4 of the AST.

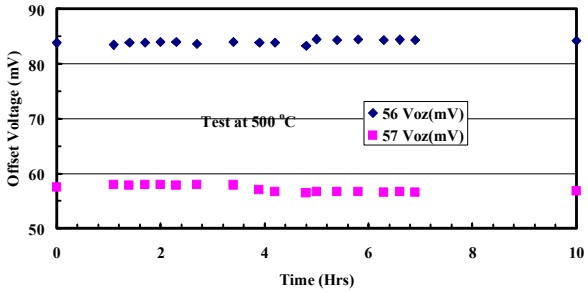

Figure 3: Time history of V_{oz}(500 °C) of two transducers after 10 hours of cyclic heating at 500 °C.

The long-term stability of the transducer zero pressure offset, V_{oz}, during Step 3 was evaluated by cyclic heating and cooling of the transducers. Figure 3 shows that after a total of 10 hours of soaking transducers 56 and 57 at 500 °C (cooling down sequences not included in total time), transducer 56 had a maximum drift of V_{oz} (500 °C, t) from V_{ozref} (500 °C) of less than 1.0 mV. In the case of transducer 57, the maximum drift from reference was less than 2 mV. For both transducers, the reference values were the values at t=0, and these

values were set after a 24-hr burn-in period at 500 °C to stabilize the transducer output.

3.0 Field validation and failure analysis

The field validation of the transducers was performed at the Sandia National Labs, where they were subjected to oil pressure up to 400 psi. During the test, the temperature was held at a fixed value, starting from 150 °C, over time, after which it was then increased by 25 °C. Table 1 shows the initial result of the test performed on transducer 56. The change in V_{oz}, ΔV_{oz}, is the maximum difference between the reference V_{oz} at the test temperature for time equal zero, $V_{ozref}(T, t=0)$. For example, it shows that ΔV_{oz} after the duration at 150 °C at 0 psi and 400 psi is 0.1 mV. This transducer was tested up to 225 °C at which it failed after 32 hours when an open circuit reading was observed. The resulting failure was manifested by a very high bridge output resistance (> 1 MΩ). Surprisingly, this was the same transducer that successfully passed the rigorous AST protocol (see Figure 3) at 500 °C.

Table 1: Thermal history of transducer 57 after soak at 225 °C shows the recorded drifts in the zero pressure offset at the beginning and end of the duration at temperature.

Duration (hrs)	Temp (°C)	0 psi	400 psi
		ΔV_{oz} (mV)	ΔV_o (mV)
Start	**20**		
130	**150**	**0.1**	**0,1**
Cool	**20**	**0.7**	**0.7**
40	**175**	**0.1**	**0**
200	**200**	**0.2**	**0.9**
32	**225**	**0**	**0.1**

To understand the failure mechanism(s), we used Auger Electron Spectroscopy (AES), Scanning Electron Microscopy (SEM), and Energy Dispersive X-ray (EDX) to perform cross section analyses of the failing transducers and other test samples, paying particular attention to the sensor bondpad/die-attach interface. The result of the AES analysis is shown in Figures 4a and b before and after sensor packaging, respectively. While Figure 4a shows a well defined reaction zone of the metal contact to the SiC, which is obtained from an unpackaged sensor, Figure 4b reveals the agglomeration of oxygen between the sensor bondpads and the die-attach after the sensors is packaged. It is believed that the high oxygen concentration at that interface acts as a dielectric layer that prevents the Au die-attach from effectively adhering to the sensor bondpad. The SEM that was performed further confirmed the AES result. In Figure 5, the SEM of the cross section of a failed transducer shows the existence of a delamination running parallel between the bond pad and the die-attach material. The EDX analysis of the delaminated region also confirmed the presence of oxygen as previously determined by AES.

With the Direct Chip Attach (DCA) technique used in packaging the SiC sensors, the hermetic sealing process requires that the sealing glass be fired to flow at 650 °C in atmosphere. This process allows the glass to wet the peripheral sides of the sensor and the aluminum nitride header, thus creating a hermetically sealed cavity. However, this process causes the glass paste to outgas into the cavity. Such outgassing causes a pressure build-up in the reference cavity, which could then push the sensor outward, thereby potentially detaching the bondpad from the die attach material. The probable occurrence of such mechanism would result in a weak bond at the die-attach/bondpad interface.

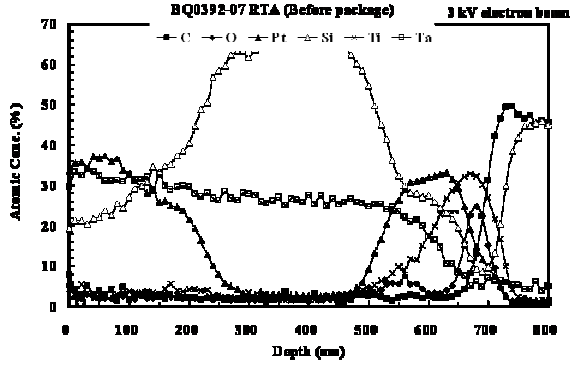

(a)

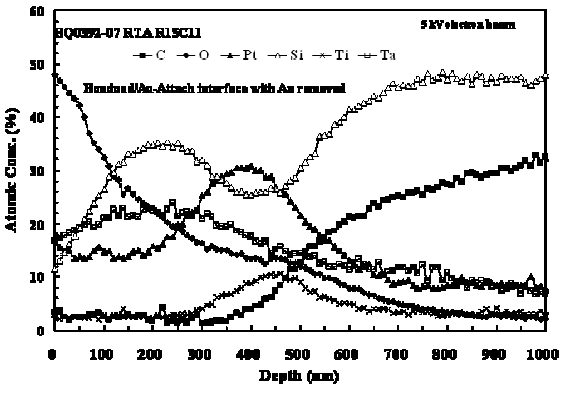

(b)

Figure 4: Representative AES of a) SiC pressure sensor bondpad annealed in nitrogen before packaging, and b) the bondpad after glass sealing. The presence of a high concentration of oxygen can be seen at the die-attach/bondpad interface. The disparity in thickness profile between Figs. 4b and 5 is due to the "tailing" effect of the sputtered thick gold die-attach during AES.

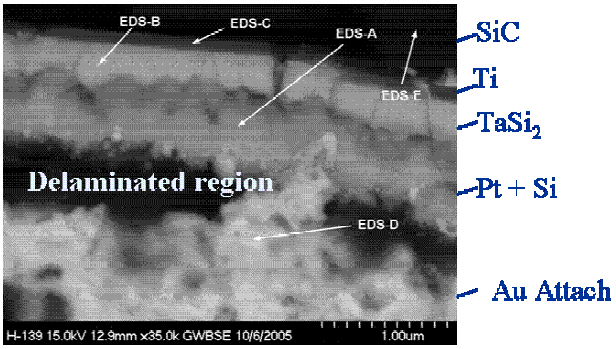

Figure 5: High resolution field emission SEM micrograph of the sensor cross section reveals the delaminated region between the die-attach/bondpad interface that could have resulted in the electrical disconnection.

Another likely mechanism is the high pressure build-up in the cavity during the atmospheric curing of the die-attach that could lead to the rapid diffusion of oxygen through the die-attach toward the sensor bondpads. However, the contact metallization was originally designed to act as a diffusion barrier against oxygen to preserve the interfacial integrity of the metallurgical junction with the SiC [9]. The result will be the agglomeration of oxygen between the bondpad and die attach material. The likelihood of such mechanism is given credence by the AES result of Figure 4b.

Systematic monitoring of the sensor resistance before and during packaging clearly showed a dramatic increase in the resistance from 1-5 kΩ to > 1 MΩ. Table 1 shows a profile of the resistance at critical steps of the packaging process. It can be seen that the dramatic increase in resistance generally occurs during the final

Table 2: Systematic evaluation of the bridge output resistance at critical steps of the packaging process. Most sensors packaged with a sealed cavity failed while most sensors packaged with open cavity passed.

Sensor #	Bare die (kΩ)	After die attach (kΩ)	After glass sealing (kΩ)	Package used
1206	2.99	2.75	3.4×10^3	Sealed Cavity
1806	4.10	3.71	10.2×10^3	"
2015	5.76	5.1	6.5×10^3	"
1006*	3.73	3.6	3.6	Open Cavity
1306	2.99	3.19	2.74	"
1506	3.28	3.02	3.23	"
1606	3.40	3.12	3.25	"

* Failed during temperature/pressure test

hermetic glass sealing process. The AES similar to the one in Figure 4b showed a high concentration of oxygen between the contact metallization and the gold die attach. The effect of this oxygen concentration was to induce a high resistance between the bondpads and the die-attach, thereby leading to a high resistance and making the sensor irreversibly unstable.

4.0 Package reconfiguration

Based on this new understanding, the sensor package was reconfigured from a sealed reference cavity to an open one. As a result, the outgassing species were able to effectively vent through the backside of the package into the atmosphere. All the sensors that were packaged after this modification exhibited very minimal changes in resistance but remained within specification, which was in sharp contrast from the sensors packaged in sealed cavities. This can be seen in Table 2, providing a direct proof that a successful solution to the problem has been found. These sensors are currently undergoing the AST and the details of the results will be reported in the future. The opening of the cavity to allow venting of the outgas means that the sensed pressure will be referenced to atmospheric pressure, which could change depending on location. Therefore, effort is underway to optimize the sealed cavity volume so that outgas can be contained while it does not adversely affect the bond integrity.

5.0 Conclusion

The reliability problems that are associated with the SiC pressure sensors have largely contributed to hinder their long-term insertion into real applications. In this work, we performed extensive FA on several SiC pressure transducers that were packaged using the MEMS-DCA approach. The hermetic sealing process was found to lead to the outgassing of the binder material in the sealing glass and the die-attach. The outgassing leads to a pressure build-up that results in degrading the die-attach/bondpad interface. Failure is thus manifested by significant increase in the output bridge resistance. The result from the FA has led to the reconfiguration of the package to allow proper venting of the outgassing species during packaging. All the sensors that were packaged after this modification exhibited very minimal changes in resistance.

5.0 Acknowledgements

This work was funded under the Technology Transfer Project at NASA Glenn Research Center. We wish to thank the technical staff of the SiC Microsystems Fabrication Laboratory at NASA-Glenn for fabrication, sample preparation, and metrology.

References

[1] Alexandar's Gas and Oil Connections, News and Trends: North America, vol. 8 Issue 13. (2003).

[2] L. G. Matus, J.A. Powell, and C.S. Salupo, "High-voltage 6H-SiC p-n junction diodes", Appl. Phys. Lett., vol. 59, pp 1770-1772, (1991).

[3] M. Khan, H. Fatemi, J. Romero, and E. Delenia, "Effect of high thermal stability mold material on the gold-aluminum bond reliability in epoxy encapsulated VLSI devices," Proc. 26th International Reliability Physics Symposium, April, 12-14, pp. 40-49. (1988)

[4] R. S. Okojie, "Characterization of 6H-SiC as a Piezoresistive Pressure Sensor for High Temperature Applications," Ph. D. Thesis, New Jersey Institute of Technology, Newark, NJ. (1996).

[5] F. Masheeb, S. Stefanescu, A. A. Ned, A. D. Kurtz, and G. Beheim, "Leadless sensor packaging for high temperature applications," The 5th IEEE Intl. Conf. Micro Electro Mechanical, pp. 392–395, Jan. 2002.

[6] R. S. Okojie, Glenn M. Beheim, George J. Saad, and E. Savrun, AIAA-2001-4652 AIAA Space 2001 Conference and Exposition, Albuquerque, NM, Aug. 28-30, 2001.

[7] http:www.jedec.org.

[8] R.S. Okojie, E. Savrun, P. Nguyen, V. Nguyen, and C. Blaha, **IEEE** Sensors, 2004. Proceedings of IEEE 24-27 Oct. 2004 Page(s):635-638 vol.2.

[9] R.S. Okojie, D. Lukco, Y.L. Chen, and D.J. Spry, J. Appl. Phys. 91, 6553 (2002)